

SCI. REP. KYOTO PREF. UNIV. (NAT. SCI. & LIV. SCI.), NO. 37, Ser. A, p. 13~19 (NOV. 1986)

Developments on the Uji Proton Microprobe

YOICHI HARUYAMA and ATSUSHI AOKI

Laboratory of Applied Physics, Kyoto Prefectural University,
Shimogamo, Sakyo-ku, Kyoto 606, Japan.

KOJI YOSHIDA and FUMIO FUKUZAWA

Department of Nuclear Engineering, Faculty of Engineering, Kyoto University,
Yoshida, Sakyo-ku, Kyoto 606, Japan.

(Received August 15, 1986)

Abstract

The Uji scanning microprobe system has been developed with two doublets configuration. A microcomputer was used for controlling the deflecting voltage dividing the scanning area of $1\text{mm} \times 1\text{mm}$ to 32×32 points and for processing RBS data in MCS mode. The beam size was reduced to $8 \times 34 \mu\text{m}^2$ with current of $\sim 1\text{nA}$.

Extraction of this micro beam through a nozzle into the atmosphere was carried out successfully.

Introduction

The scanning MeV ion beam technique combined with PIXE and RBS is very useful for the measurements of spatial concentration distributions of trace elements because of its high sensitivity and spatial resolving power for bulk samples.

In the previous paper¹⁾, the authors reported that the microbeam was easily produced by the simple slit system. However, this method was not practical for the trace element analysis because the beam currents decreases with reduction of the beam size. Usually to focus MeV ion beams, quadrupole lenses are used. As quadrupoles have asymmetric focussing properties, more than two of them are combined to form a lens. The configuration of quadrupoles is classified by the number of singlet, i. e., doublet²⁾, triplet³⁾ and quadruplet⁴⁾. The microbeam apparatus is installed to 4 MV van de Graaff accelerator at Uji, Kyoto University. Since divergence of the beam is rather wide ($\sim 2\text{mrad}$ in the vertical plane), two doublet configuration is adopted to pre-focus the diverging beam and to focus it on the target.

In the present paper, the two doublets configuration and some improvements on scanning and data handling system are described. And a preliminary experiment on the external microbeam is reported.

Experimental

The experimental set-up of the Uji scanning microprobe apparatus is shown in Fig. 1. The energy analysed MeV proton beam is pre-focussed by the first doublet (Q1 and Q2) to suppress the beam divergence. The beam was collimated by the crossed slits less than $1\text{mm} \times 1\text{mm}$. Finally, the second doublet (Q3 and Q4) focussed the beam on the target plane. Geometric parameters of two quadrupoles

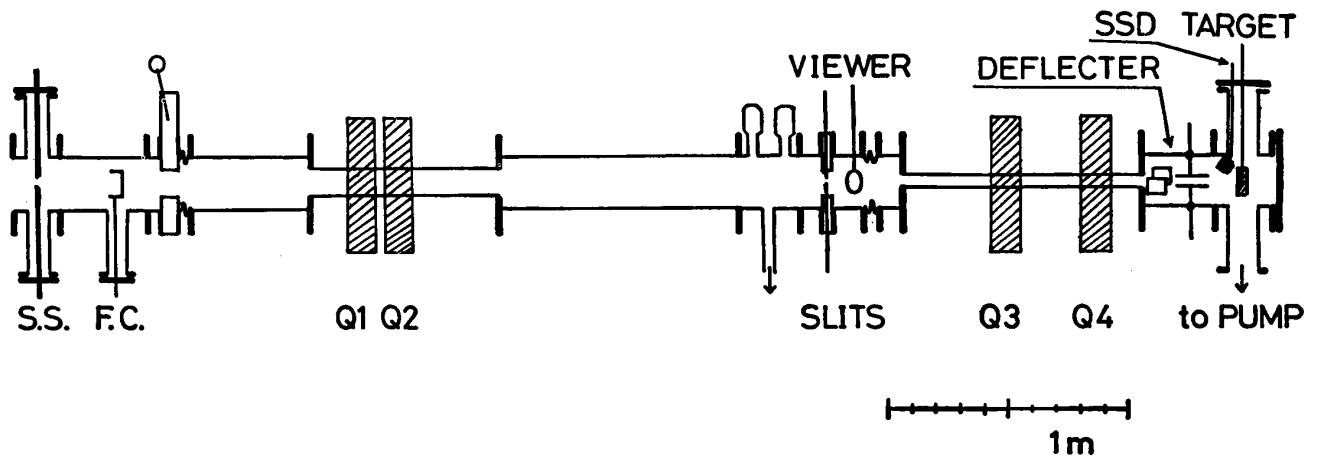


Fig. 1. The experimental set-up of the Uji microprobe.

Table 1 Geometric parameters of quadrupoles

	Q1, Q2	Q3, Q4
bore radius	30mm	10.5mm
pole radius	30mm	12.5mm
pole length	120mm	140mm
coil winding	825 turn	265 turn
material	SS	pure iron

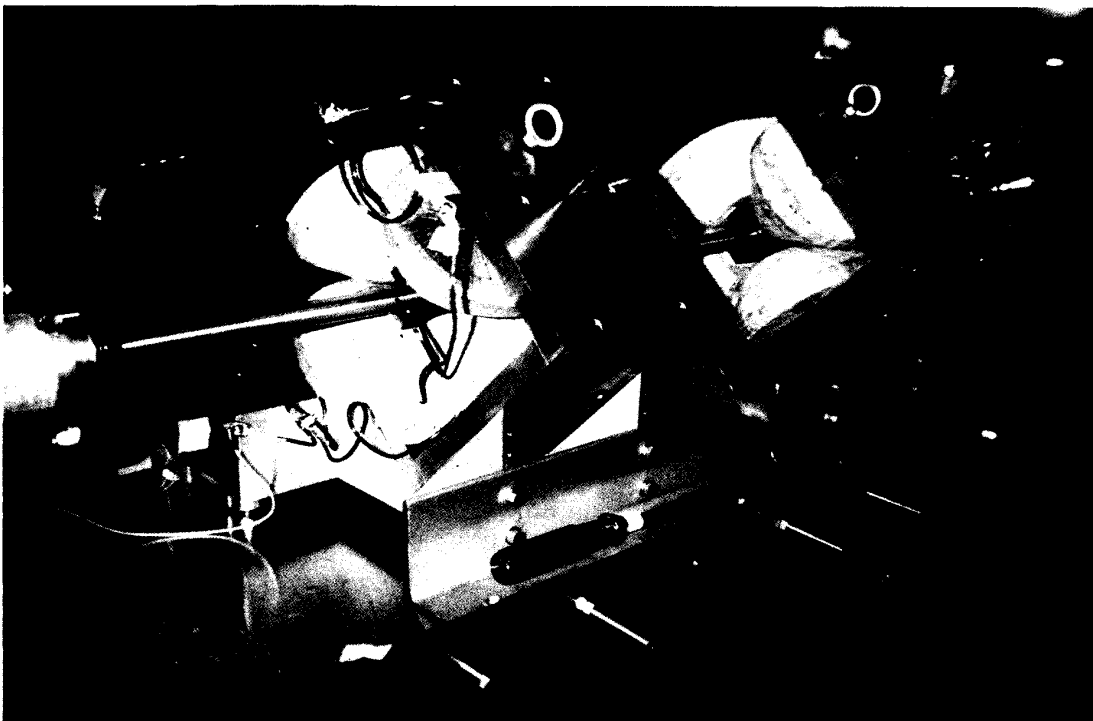


Fig. 2. A view of the second quadrupole lenses on their supports.

are tabulated in table 1. Each quadrupole lens has rectangular yoke mounted on a support V block. The position and the direction of the quadrupole was adjusted easily by the free bearings connected with the V block (see Fig. 2). Each lens axis was carefully aligned to the beam axis and it took almost one

day.

In order to minimize the beam size, the light spot on a glass plate at the target position was observed with a microscope placed after the target. The surface barrier semiconductor detector (SSD) was positioned approximately 40 mm apart from the target at an angle of about 135°. Beam deflection electrodes (deflector), mounted between the second quadrupoles and the target, enable the beam to be scanned over the target.

In the present experiment, a microcomputer was used for controlling the microbeam. The block diagram of the scanning system is illustrated in Fig. 3 together with the data handling system. Deflection voltage data were fed to digital to analog converter (DAC) through peripheral interface adapter (PIA) by the microcomputer (FM-8) producing saw-tooth wave forms as depicted in Fig. 3. The wave forms were amplified to 1 kV amplitude by high voltage amplifier (HSR-1. 1P-L35 ; Mastusada precision devices) and were fed to the beam deflection electrodes. The spatial resolving power was restricted by the memory capacity of the microcomputer and data length of the PIA (8bits/direction). Usually 256 points for one dimension scanning and 32×32 points for two dimensions were adopted. The dwell time at each points in the raster is determined by counting the number of the clock pulses (100 Hz) generated by the clock. It was usually one second.

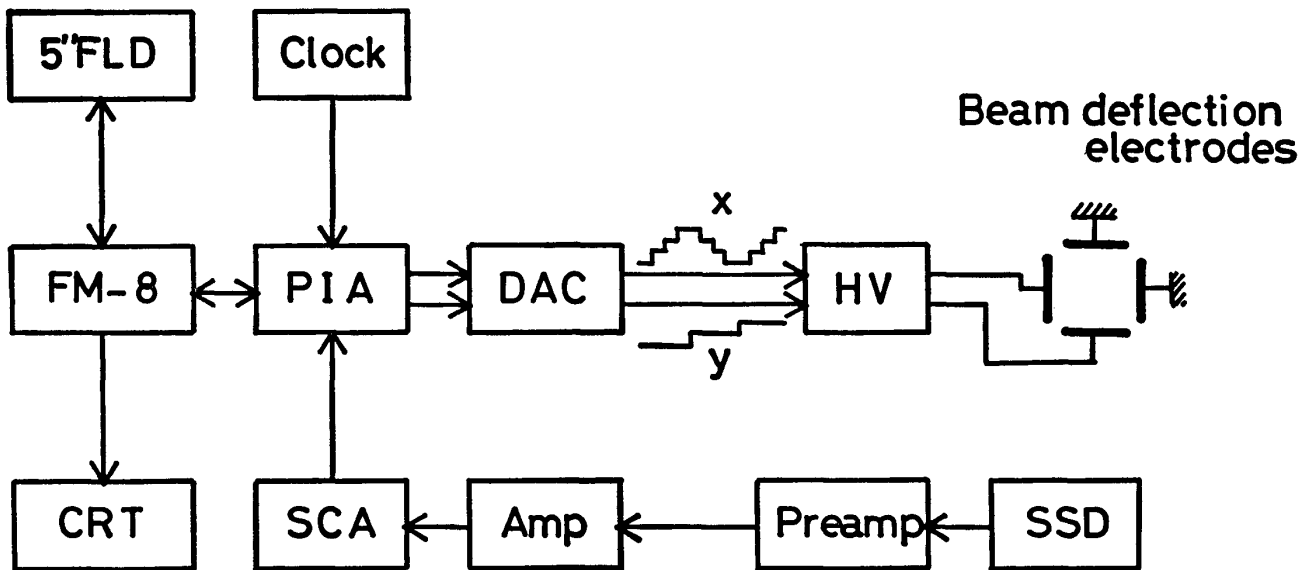


Fig. 3. Schematic diagram of the scanning and data acquisition system.

The backscattered protons were detected by the SSD. The microcomputer counted the number of energy gated pulses corresponding to the element concerned, stored in the memory and displayed it in one or two dimensional image on CRT. These data were transferred to FLD and analysed after scanning.

In order to analyse the beam trajectory, a simple program has been developed for the first order approximation. The equations of motion of a charged particle in a magnetic field \mathbf{B} are

$$-\frac{d}{dt}(m\mathbf{v}) = q\mathbf{v} \times \mathbf{B}$$

where q is the charge, m is the mass and v is the velocity of the particle. By neglecting the field component and small change of ion velocity along with the beam axis, (z axis), these equations reduce to

$$\frac{d^2x}{dt^2} = -(qv/m)B_y$$

$$\frac{d^2y}{dt^2} = (qv/m)B_x$$

Changing the independent variable from t to z , one can obtain

$$\frac{d^2x}{dz^2} = -\frac{q}{mv} B_y$$

$$\frac{d^2y}{dz^2} = \frac{q}{mv} B_x$$

The magnetic potential of quadrupole is represented by the form as the first order approximation,

$$\phi_m(x, y, z) = \frac{2\mu_0 NI k(z)}{a^2} xy$$

where μ_0 is the permeability of vacuum, NI is the magnetomotive force, a is the bore radius and $k(z)$ is the strength of the field along with z axis. We adopted the rectangular distribution of the magnetic fields, that is, $k(z)$ is unity inside the effective length of the quadrupole lens and zero outside.

Then, one can obtain the differential equation with respect to the z as follows,

$$\ddot{x} + \beta^2 x = 0$$

$$\ddot{y} - \beta^2 y = 0$$

where β^2 is $(q/mv) (2\mu_0 NI/a^2)$. In matrix notation, the position and the velocity of the ion at the exit of the lens of effective length l are written as

$$\begin{pmatrix} x \\ x' \end{pmatrix} = \begin{pmatrix} \cos\beta l & \beta^{-1}\sin\beta l \\ -\beta\sin\beta l & \cos\beta l \end{pmatrix} \begin{pmatrix} x_0 \\ x'_0 \end{pmatrix}$$

$$\begin{pmatrix} y \\ y' \end{pmatrix} = \begin{pmatrix} \cosh\beta l & \beta^{-1}\sinh\beta l \\ \beta\sinh\beta l & \cosh\beta l \end{pmatrix} \begin{pmatrix} y_0 \\ y'_0 \end{pmatrix}$$

under the initial condition of x_0, x'_0, y_0, y'_0 at the entrance. The beam trajectory was simulated with a computer using the above equations and is shown in Fig. 4.

The experimental arrangement for an external microbeam system after the second doublet is shown

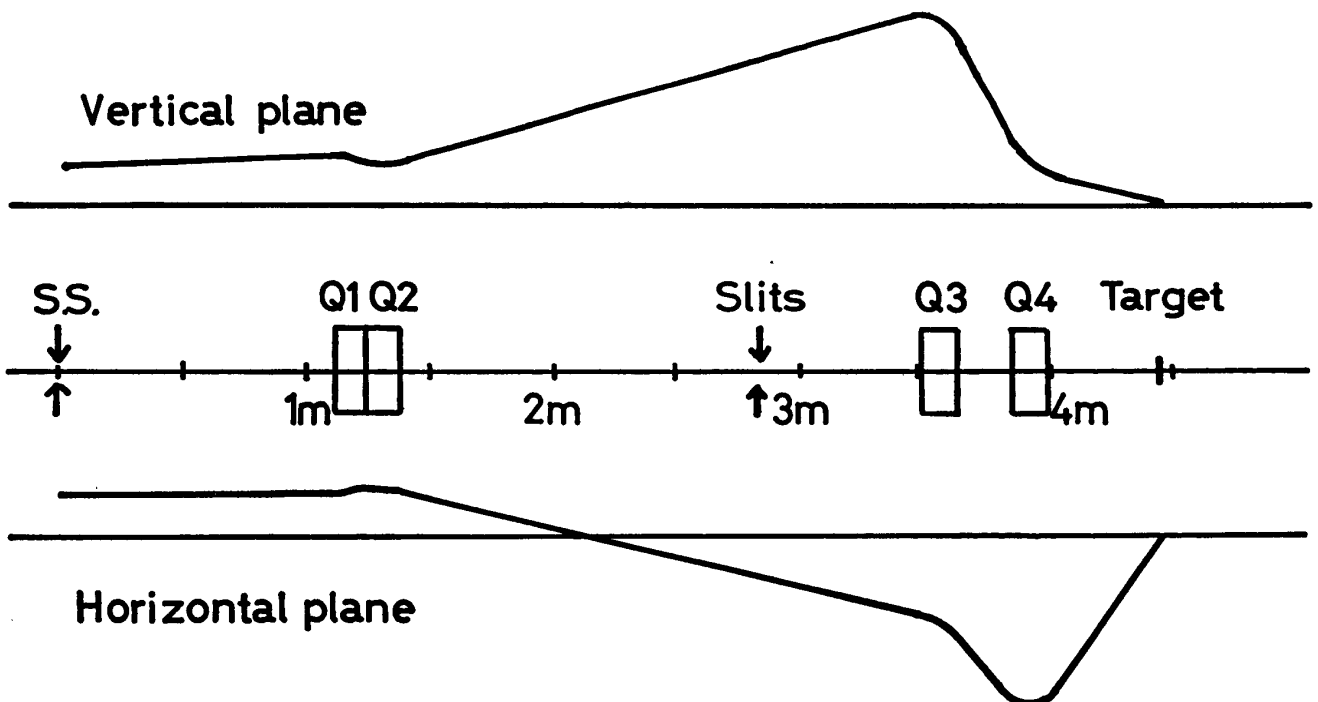


Fig. 4. The calculated path of the beam in the vertical and horizontal planes.

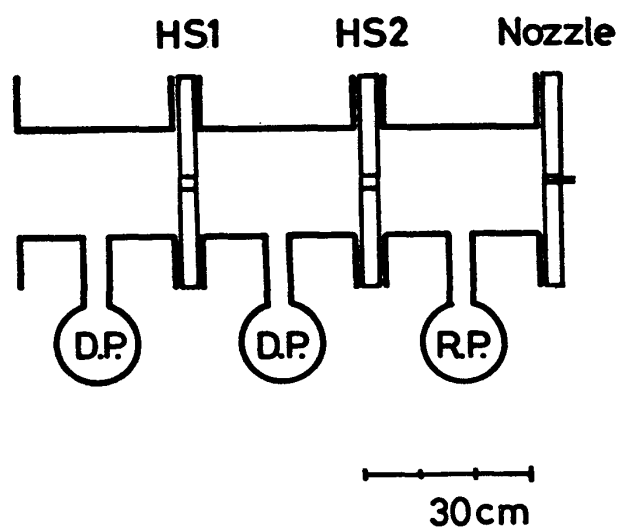


Fig. 5. The experimental set-up for the external beam. HS 1 and HS 2 are the hole slits of $1\text{ mm}\phi$ and 20 mm in length. The exit nozzle is $0.16\text{ mm}\phi$ in diameter and 20 mm in length.

in Fig. 5. To extract the beam into the atmosphere, the beam duct was evacuated by the triple differential pumping with two 2" oil diffusion pumps (D.P.) and a rotary pump (R.P.). The hole slits (HS 1 and HS 2) of $1\text{ mm}\phi$ and 20 mm in length were used and the injection needle made of stainless steel of $0.16\text{ mm}\phi$ and 20 mm in length was used as the exit nozzle. The typical pressures in the beam duct were 10^{-5} , 10^{-3} and 10^{-1} Torr, respectively. The main use of the quadrupoles was in increasing the intensity of the microbeam by an order of magnitude.

Results and discussion

In the present experiment, 2 MeV proton beam was used. The focussed beam size was measured by RBS scan of a 150 lines/inch copper electron microscope grid. Two dimensional RBS picture is shown in Fig. 6. The grid lines were measured by using an optical microscope to be $40\mu\text{m}$ in width and the repeat distance $170\mu\text{m}$. Scanning area covered $0.75\text{ mm} \times 1\text{ mm}$ and was divided in 32×32 points. The dwell time at each point in the raster was 3 seconds. Due to a trouble of the accelerator during the scan, some data points were lost as is seen in Fig. 6. In order to determine the beam size, two dimensional scanning data reduced to one dimensional ones. In Fig. 7 (a) and 7 (b), are shown the horizontal and vertical scanning spectrum, respectively. Due to the fluctuation of the beam intensity and poor spatial resolution (32 points/mm), the measured FWHM of the peak had some uncertainties. They were $48 \pm 8\mu\text{m}$ and $74 \pm 10\mu\text{m}$, respectively. The beam size is estimated from these values and the grid width to be $8 \pm 4\mu\text{m}$ and $34 \pm 10\mu\text{m}$, respectively. The intensity of this focussed beam was not measured directly, however, it was estimated to be the order of nA from the area defined by the slits and the intensity of the original beam.

A few problems are revealed through the present experiment. For an analytical purpose, the dwell time at each point should be determined from integrated beam currents in order to avoid the influence of a fluctuation of the beam intensity. A beam steering system should be installed, because misalignment of the lenses was caused by a slight change of the beam course during the experiment.

Extraction of the microbeam through the nozzle into the atmosphere was carried out successfully. The result of the external beam is shown in Fig. 8. The light spot on the glass plate is clearly seen.

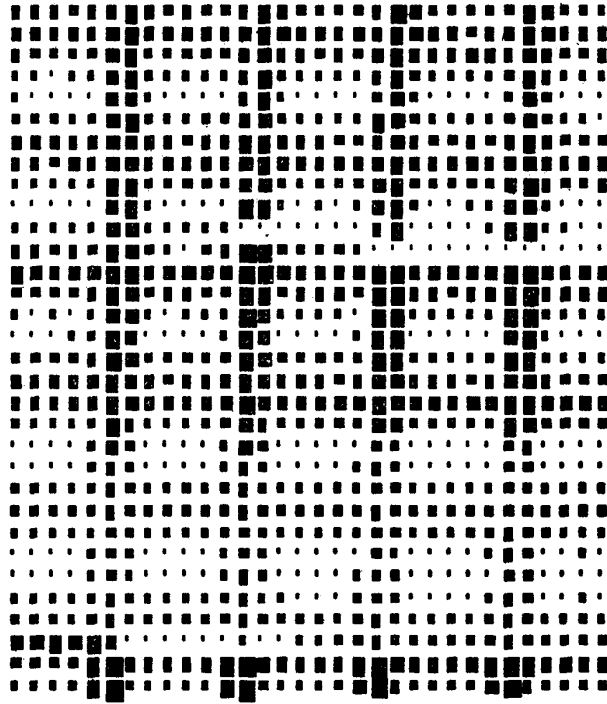


Fig. 6. Two dimensional image of RBS scan of 150 lines/inch copper electron microscope grid. The grid lines are $40\ \mu\text{m}$ in width and the repeat distance is $170\ \mu\text{m}$.

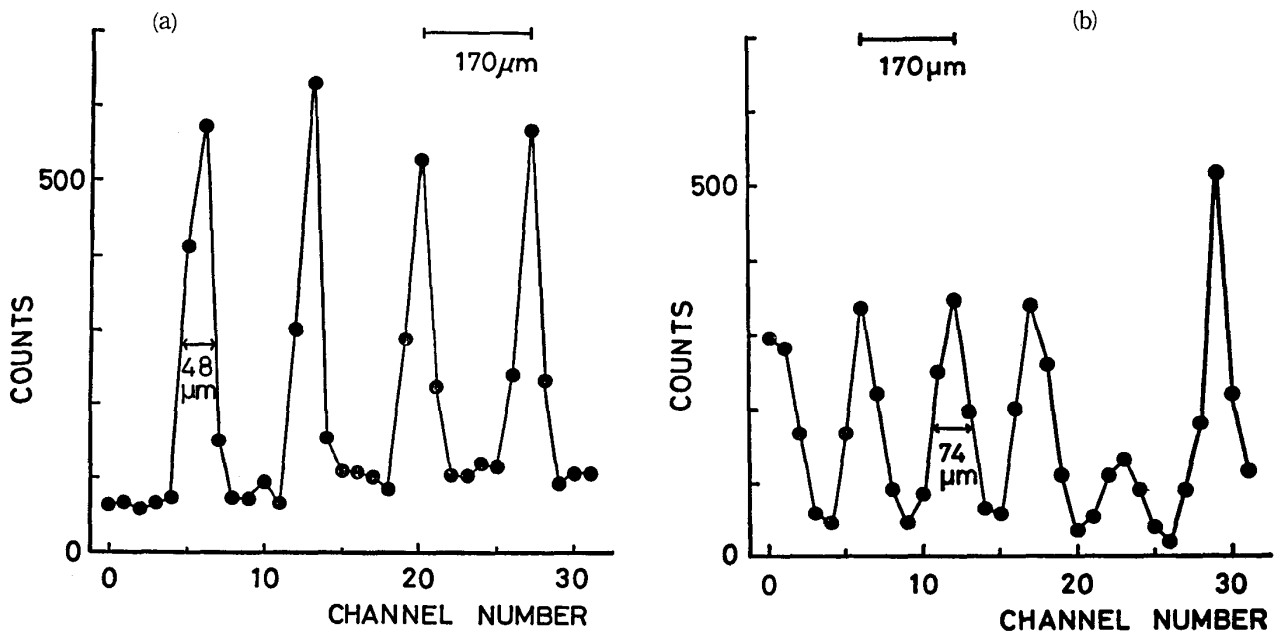


Fig. 7. Spectrum of backscattered protons in (a) horizontal and (b) vertical scanning.

As this experiment was only a preliminary one, the beam size and current were not measured.

A convenient microbeam system for laboratory use was developed with remarkable low cost compared with other facilities. This microbeam of order of $10\ \mu\text{m}$ is expected to be applied to many fields, such as biology, medicine, material science, metallurgy, archaeology and so on.

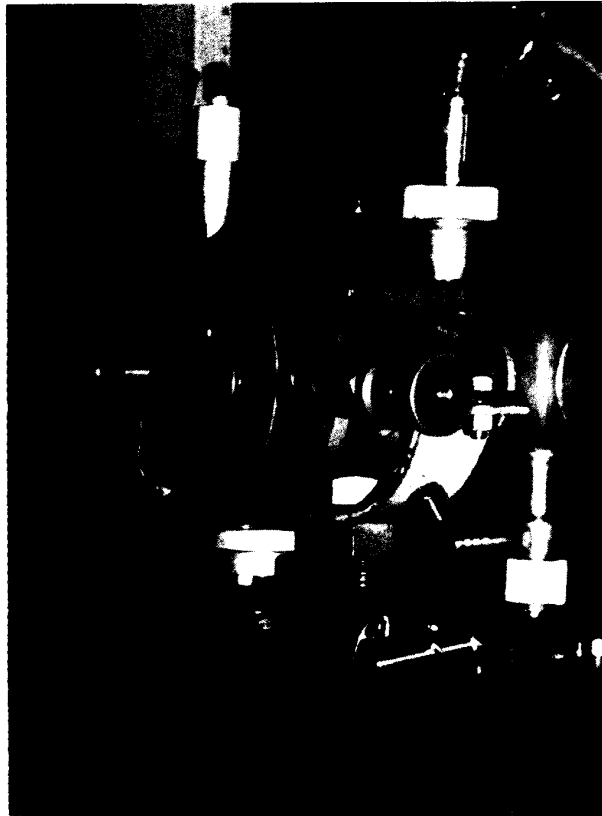


Fig. 8. A view of the external microbeam system.
A light spot on the glass plate is seen.

The authors wish to express their gratitude to Mr. K. Norizawa for his kind advice in preparing electronic circuit for microbeam scanning and data handing.

References

- 1) Y. Haruyama, A. Aoki, K. Yoshida and F. Fukuzawa, *Sci. Rep. Kyoto Pref. Univ. (Nat. Sci. & Liv. Sci.)*, **36**, (1985) 9-13
- 2) H. Kneis, B. Martin, R. Nobile, B. Povh and K. Traxel, *Nucl. Instr. Meth.* **197**, (1982), 79-83
- 3) F. Watt, G. W. Grime, G. D. Blower and J. Takacs, *Nucl. Instr. Meth.*, **197**, (1982), 65-77
- 4) G. J. F. Legge, D. N. Jamieson, P. M. J. O'Brien and A. P. Mazzolini, *Nucl. Instr. Meth.*, **197**, (1982), 85-89